Theoretical Study of Adsorption of Water Dimer on the Perfect MgO(100) Surface: Molecular Adsorption versus Dissociative Chemisorption

Yan Wang[†] and Thanh N. Truong*

Henry Eyring Center for Theoretical Chemistry, Department of Chemistry, University of Utah, 315 S 1400 E, Room Dock, Salt Lake City, Utah 84112

Received: October 29, 2003; In Final Form: January 5, 2004

We present a theoretical study on the mode of adsorption of the water dimer on the perfect MgO(100) surface using the ab initio embedded cluster method. Structures and normal-mode analyses were carried out at the HF level of theory, while energetic information was improved using the IMOMO methodology at the CCSD level using a smaller model system. We found that a single coadsorbed water molecule nearby can stabilize the hydroxyl species resulting from dissociation of the adsorbed water. The dissociative product is less stable by 25.5 kJ/mol compared to the molecular adsorbed water dimer. Since the reverse barrier is only 3.8 kJ/mol and is removed when zero-point energy correction is included, hydroxyl species would not be observed for the adsorption of a water dimer. Analysis on the degree of stabilization due to the coadsorbed water molecule suggests that two or more coadsorbed water molecules would yield observable hydroxyl species. These results support recent MIES experimental evidence of water dissociation on the perfect MgO(100) surface in the submonolayer regime. Our results also indicate that the effects of the Madelung potential are significant for studying chemisorption processes on ionic metal oxide crystal surfaces.

Introduction

Adsorption of water on a MgO(100) oxide surface has been a subject of many experimental and theoretical studies due to its importance in geochemistry and heterogeneous catalysis.[1−8] In particular, MgO is a principal component of many minerals found in the Earth's subsurface. Thus, interaction of water with MgO surfaces affects the hydrodynamic properties of the Earth's subsurface. From a surface science point of view, MgO(100) has been used as a model system for understanding fundamental interaction with oxide surfaces due to its simple and well-characterized surface structure.[9−20] Despite the fact that numerous experimental and theoretical studies have been done, fundamental understanding on the mode of adsorption of water on the MgO(100) surface is still not complete and many remaining issues have not yet been addressed—in particular, factors that affect the mode of adsorption of water, namely, molecular adsorption versus dissociative chemisorption on the MgO(100) surface.[21−24] It is a well-accepted fact from many experimental and theoretical studies that isolated water only adsorbs molecularly on the perfect surface and may dissociate at defect sites.[3,25−32] In addition, it is known that the MgO(100) surface is hydroxylated at the solid−liquid water interface.[9,33−35] Although it was initially suggested that such hydroxylation initiates at defect sites, our recent theoretical study in collaboration with metastable impact electron spectroscopy (MIES) experiments done by Goodman and co-workers[36] concluded that hydroxylation can occur on the perfect MgO(100) surface. This raises the question on the importance of coadsorption effects.

Recently, Kim et al.[36] reported an experimental study using the metastable impact electron spectroscopy (MIES), ultraviolet photoelectron spectroscopy (UPS), and temperature-programmed desorption (TPD) technique that provides first evidence that water adsorbed on the perfect MgO(100) surface can dissociate partially within the first monolayer. This support results from several previous theoretical studies using periodic electronic structure methods.[33,37−39] In particular, it was suggested that the perfect MgO(100) surface facilitates the formation of an extended 2D hydrogen-bond network from water molecules that partially covered the surface.[39,40] Such a network stabilizes the dissociation products, i.e., the hydroxyl species. Furthermore, from these theoretical studies two different dissociation models were proposed:[34,38,41] in one-half of water molecules in a (2×2) monolayer and in another one-third of water molecules in a (3×2) monolayer are dissociated. Though the latter model was found to fit better with MIES spectra of 1.4 L water on the perfect MgO(100) surface. In addition, on the basis of ab initio molecular dynamics simulations, Giordano et al.[42] suggested that water dissociated on the MgO perfect surface may easily desorb in the molecular form. A cluster model was also been used by Almeida et al.[28,29,33] to study the coadsorption effects on the water adsorption properties. Due to the cluster size being used, the results provided interesting insight into the reactivity of different structural defects. However, the much larger predicted binding energy of a single water molecule on a perfect MgO(100) surface Mg site of 167.6 kJ/mol compared to TPD experimental data of about 62.8 kJ/mol indicates that edge effects may be large and can greatly affect the calculated properties for adsorption of water on the perfect MgO(100) surface. Furthermore, the effect of the Madelung potential was not included in these cluster studies, but was found in this study as discussed later to be rather important for stabilizing the transition state to water dissociation and the dissociated product. As of this date, a reaction path for water dissociation on the perfect MgO(100) has not been reported.

From the above discussion, it is clear that coadsorbed water molecules promote the dissociation process. However, how

* Corresponding author. E-mail: Truong@chemistry.utah.edu.
[†] On leave from Department of Chemistry, Beijing Normal University, Beijing 100875, P. R. China.

10.1021/jp031195a CCC: $27.50
Published on Web 02/14/2004

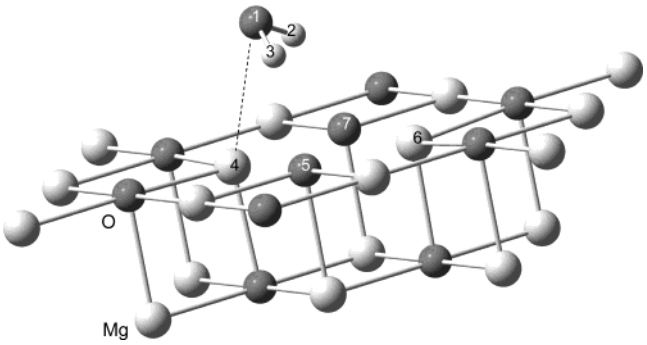

Figure 1. Structure of isolated water molecule adsorption on the MgO(100) surface. The $Mg_{18}O_{10}$ cluster shown is treated quantum mechanically in the embedded cluster model.

important is the extended hydrogen-bond network, which implies the long-range effects, in facilitating such a process? Would local hydrogen-bonding from a cluster of two or three water molecules adsorbed on the perfect MgO(100) surface be sufficient to form hydroxyl species? How stable would such a species be, if it existed? If so, there also exists a transition state that connects the molecular adsorbed and the dissociative chemisorbed states. What would be the activation energy for such a process? How important is the Madelung potential in facilitating this process? These are different questions designed to address the importance of the local hydrogen-bond effects. Addressing these questions is the main objective of this study. To do so, we have employed an ab initio embedded cluster method to examine the potential energy surface of the water dimer adsorbed on the perfect MgO(100) surface. Using the embedded cluster approach allows us to model only the local hydrogen-bond interactions instead of the extended network as in a periodic method. Thus, comparing our results with those from previous calculations would provide insight into the roles of coadsorption effects.

Computational Details

We employed the Surface Charge Representation of the External Embedding Potential (SCREEP)[21] method to model interactions of the water dimer with the MgO(100) surface. The MgO(100) surface consists of a quantum cluster $Mg_{18}O_{10}$ as shown in Figure 1 surrounded by a set of pseudopotentials for all Mg^{2+} ions that are nearest to any quantum oxygen atom and a set of point charges, whose unit cell was within 1.2 nm from any of the quantum cluster atoms. These pseudopotentials and point charges are located at the lattice positions. The effects of the remaining Madelung potential is represented by a set of surface charges derived from the SCREEP methodology. More details on the SCREEP method can be found elsewhere.[22,43−45] HF was used with a mixed basis set to optimize selected geometrical parameters of all stationary and saddle points for the adsorption and dissociation paths of water on the perfect MgO surface. In particular, the 6-31G(d, p) basis set was used for the water dimer, and for selected surface Mg and O atoms (atom number 4, 5, 6, and 7) close to the adsorption site as shown in Figure 1. The 3-21G (d, p) basis set was used for the remaining cluster atoms. Normal-mode analysis was carried out for the transition state to confirm the eigenvector of the imaginary frequency corresponding to the water dissociation pathway. To improve the energetic properties, we also employed the IMOMO (integrated molecular orbital + molecular orbital) method.[44,45] The IMOMO method allows interactions in a subregion of the system to be treated at a more accurate level of theory and thus provides a cost-effective method for improving accuracy of the calculated properties. In this case, a smaller quantum cluster consisting of the adsorbed water dimer and surface atoms Mg4, O5, Mg6, and O7 were selected as a model system and were treated at the CCSD/6-311+G(d,p) level. The interaction energies have been corrected by the basis set superposition error (BSSE) using the counterpoise method within the IMOMO formulation for calculating the total energy.[46] The IMOMO method was found to be quite useful for improving energetic properties in our previous study of adsorption on metal oxide surfaces.[45] All calculations were carried out by using the Gaussian98 program.[47]

TABLE 1: Relaxation of the Four Surface Atoms (nm), Structural Parameters (nm and deg), and Binding Energy (kJ/mol) of an Isolated Water Adsorption on the MgO(100) Surface

	parameters				E_{bind}		
	Mg4	O5	Mg6	O7	HF	IMOMO	expt[51]
ΔX	0.0047	0.0002	−0.0030	−0.0027	69.68	86.48	∼63
ΔY	−0.0047	0.0028	0.0028	−0.0003	58.06[a]	74.86[a]	
ΔZ	−0.0007	−0.0007	−0.0118	−0.0008		58.02[b]	

O1−Mg4	H2−O1	∠H2O1Mg4	∠H2O1H3
0.246	0.095	73.0	104.5

[a] Zero-point energy corrected value using HF frequencies scaled by a factor of 0.9. [b] Zero-point energy and BSSE corrected value.

Results and Discussion

1. Isolated Water Adsorbed on the Perfect MgO(100) Surface. Adsorption of an isolated water on the perfect MgO(100) surface has already been well studied.[9,12,40,48] In this study, we used this system to validate the accuracy of the embedded cluster model and the level of theory being used. It is known that isolated water molecules only adsorb molecularly on the perfect MgO(100) surface. In fact, we did not find any dissociative pathway. For the molecular adsorbed state, we optimized the geometry of the adsorbed H_2O molecule and of the four surface atoms (Mg4, O5, Mg6, and O7) near the adsorption site using the HF/6-31G(d, p) method. The structure of the four surface atoms and adsorbed water is shown in Figure 1 and the adsorption properties are listed in Table 1 along with those from previous theoretical studies and available experimental data. Surface relaxation upon adsorption of a water molecule was found to be negligible. Consistent with results from FTIR experiments done by Goodman et al.[35,49] and from calculations done by McCarthy et al.[48] and by Tikhomirov et al.,[40] i.e., the adsorbed water molecule is aligned nearly parallel with the two hydrogen atoms tilting slightly toward the surface. In particular, the oxygen atom of H_2O is almost on top of the magnesium atom (Mg4) with the distance of 0.246 nm, while the two hydrogen atoms point toward the surface oxygen atoms O5 and O7 with the distance of about 0.199 nm. The calculated binding energy is 58.02 kJ/mol by using the IMOMO method with the inclusions of a zero-point energy correction of 18.56 kJ/mol using scaled HF frequencies and the BSSE correction of 16.84 kJ/mol. Note that the BSSE correction is within the range of (9.6−19.2 kJ/mol) from previous calculations using a similar level of theory.[50] The calculated binding energy from this work is consistent with the reported TPD experimental results (∼63 kJ/mol)[51,52] and previous theoretical data (59.4−73.2 kJ/mol).[9,48] These results indicate that the embedded cluster model and the level of theory used in this study are sufficiently accurate to describe interactions of water with the perfect MgO(100) surface.

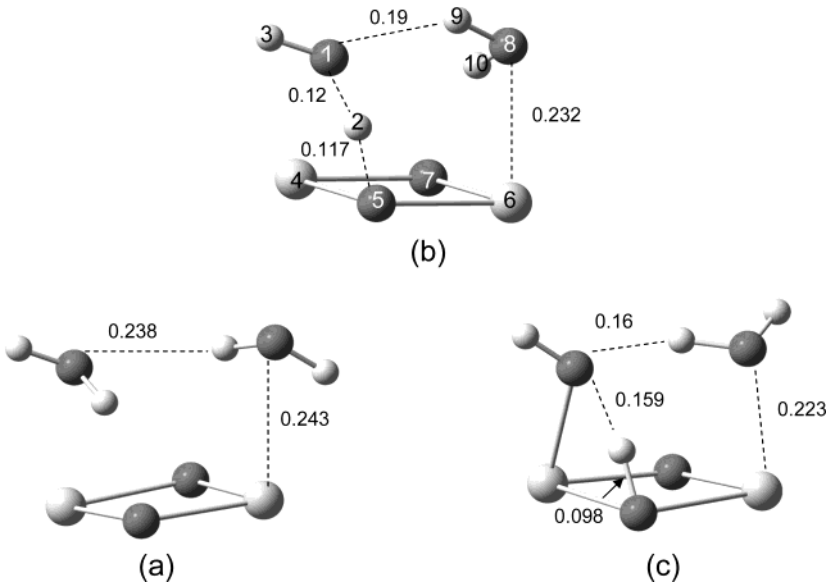

Figure 2. Optimized structures for (a) the molecular adsorbed water dimer; (b) transition state to dissociation; (c) dissociated complex on the MgO (100) surface. Selected bond distances (nm) are also given.

TABLE 2: Structural Parameters (nm and deg) of Water Dimer at Stationary Points along the Dissociative Chemisorption Pathway, Binding Energy of Water Dimer (kJ/mol), and Forward and Reverse Barriers (kJ/mol) of Water Dimer Dissociation on the Perfect MgO(100) Surface

	parameters			E_{bind}		$\Delta V_f^{\neq}$		$\Delta V_r^{\neq}$	
	R	TS	P	HF	IMOMO	HF	IMOMO	HF	IMOMO
O1−Mg4	0.243	0.223	0.208	125.15	175.02	28.55	29.26	19.69	3.80
H2−O1	0.096	0.120	0.159	106.59[a]	156.46[a]	18.94[a]	19.60[a]	12.08[a]	−3.80[c]
O1−H3	0.094	0.094	0.094		132.88[b]				
H2−O5	0.236	0.117	0.098						
H2−O8	0.240	0.269	0.248						
H9−O1	0.238	0.190	0.160						
O8−Mg6	0.243	0.232	0.223						
∠H2O1H3	108.3	115.3	124.3						
∠H9O8O10	107.3	101.3	108.4						
∠H3O1Mg4	112.9	104.2	119.0						
∠O1H2O5	140.7	164.6	156.0						
∠H9O8Mg6	83.8	111.9	101.5						
∠H10O8Mg6	66.8	76.9	111.2						
∠H10O8H9O1	142.9	37.4	144.9						
∠H3O1H2O5	112.6	95.0	112.2						
∠H10O8H9Mg6	63.3	80.2	117.1						
∠H2O5Mg6O7	−65.3	−64.3	−67.9						

[a] Zero-point energy corrected value using HF frequencies scaled by a factor of 0.9. [b] Zero-point energy and BSSE-corrected value. [c] There is not a reverse barrier due to the zero-point energy correction using HF frequencies.

2. Dissociation of Water Dimer on the Perfect MgO(100) Surface. Previous theoretical study suggested that for (3 × 2) monolayer coverage 1/3 of water molecules can dissociate, and it is supported by experimental observation.[36,38,34,41] Lynden-Bell et al.[34] also found that half of the water molecules in a (2 × 2) monolayer can dissociate to form a stable configuration. A general observation is that each hydroxyl ion is stabilized by three hydrogen bonds. As mentioned earlier, the hydrogen-bond network is crucial for stabilizing the hydroxyl species. These studies were done using periodic electronic structure methods for coverage from 0.5 to 1 ML. In this study, we found that even at lower coverage, such as a water dimer, the potential energy surface exhibits a dissociative pathway with a small reverse barrier. The hydroxyl ion is stabilized by hydrogen bonding with its coadsorbed water molecule. Below are the analyses of the water dissociation pathway.

2.1. Structures. Optimized geometries of the reactant (water dimer adsorption complex), product (hydroxyl species stabilized by a water molecule on the MgO surface), and the transition state are shown in Figure 2 with selected optimized geometrical parameters listed in Table 2.

For the water dimer adsorption complex, the two water oxygen atoms are located nearly on top of the two magnesium atoms (Mg4 and Mg6) at the distance of 0.212 nm above the MgO surface. This compares well with the previously reported value of 0.208 nm from the experiments and of 0.211 nm from periodic DFT calculations for the average distance above the surface of the water oxygen atoms.[39,52] Note that the MgO distances reported in Table 2 are slightly longer than the heights above the surface and the water oxygen atoms are not exactly on top of the Mg atoms. The distance between the two water oxygen atoms is 0.299 nm. This is not much different from 0.298 nm of the isolated water dimer. However, the hydrogen atoms of the adsorbed complex are pointing toward the surface oxygen atoms rather than forming hydrogen bonds with the coadsorbed water. Note that the two water molecules maintain a C_2-axis symmetry on the MgO surface, which agrees with previous theoretical finding.[39] For the transition state (TS), the

dissociated hydrogen atom (H2) moves toward the nearby surface oxygen atom (O5) with the distance (R_{H2O5}) of 0.117 nm. The distance (R_{H2O1}) between the same hydrogen atom (H2) and the oxygen atom (O1) of the dissociated water molecule is 0.120 nm. Normal-mode analysis confirmed that this TS was corresponding to the dissociation of one of the two adsorbed water molecules. For the product, the coadsorbed water maintains its molecular nature though it moves closer to the surface by about 0.020 nm. The OH ion binds to the Mg atom with the bond distance of 0.208 nm whereas the H ion binds to the surface oxygen with the bond distance of 0.098 nm (R_{H2O5}). This OH bond distance compares well with the previously reported values of 0.103 nm from Suzanne et al.[39] and of 0.095 nm from our previous work[9] for MgO(100)−liquid water interface.

Analyzing the variation in the water dimer structure along with the dissociation pathway provides further insights into the dissociation mechanism of water on the MgO surface. Proceeding from the reactant, adsorbed water dimer, to the dissociated product, the two oxygen atoms of the water dimer do not move noticeably on the surface (*xy*) plane from their initial adsorption positions nearly on top of the surface magnesium atoms, Mg4 and Mg6. However, their relative heights above the surface gradually decrease. In particularly, the distance (R_{O1Mg4}) between the oxygen atom (O1) of the dissociated water and the magnesium atom (Mg4) of the MgO surface decreases from 0.243 to 0.208 nm. While the distance (R_{O8Mg6}) between the oxygen atom (O8) of the coadsorbed water and the magnesium atom (Mg6) of the MgO surface only decreases from 0.243 to 0.223 nm. The large change in the O1Mg4 bond distance of the oxygen atom (O1) of the dissociated water and the magnesium atom (Mg4) on the MgO surface is expected since the dissociated hydroxyl species is forming a bond with the surface Mg atom. The spectator OH bond (O1−H3) as expected remains nearly constant along the reaction path. In addition, the hydrogen bonds of the water dimer exhibit interesting variations along the dissociation pathway. In particular, the distance between the dissociated hydrogen atom and the oxygen atom of the neighboring water (R_{H2O8}) shows small variations, namely from 0.240 nm at the reactant to 0.269 nm at the TS then to 0.248 nm at the product. However, the distance between the oxygen of the dissociated water and the hydrogen of the neighboring water (R_{H9O1}) decreases significantly and monotonically from 0.238 nm at the reactant to 0.160 nm at the product. Furthermore, these variations also cause an unusual rotation of the coadsorbed water relative to the surface. Particularly, the dihedral H10O8H9O1 decreases from 142.9° at the reactant to 37.4° at the TS then increases to 144.9° at the product. These results indicate that the coadsorbed water plays rather active roles in stabilizing both the transition state and the dissociated product, hydroxyl species.

2.2. Energetics. For discussion on the energetics of the chemisorption of the water dimer on the MgO(100) surface, we use only our most accurate results, namely the IMOMO (CCSD(cluster):HF (embedded cluster)). The differences between the HF and CCSD results for the cluster model will provide information on the electron correlation effects, and the differences between the HF results for the cluster and embedded cluster models to yield the effects of the long-range Madelung potential.

The calculated binding energy of the water dimer adsorbed on the MgO surface is 132.88 kJ/mol. This yields the average binding energy per water molecule 66.42 kJ/mol, which is 8.4 kJ/mol larger than the binding energy of 58.02 kJ/mol for adsorption of an isolated water molecule. Using the 3 × 2 water monolayer model on the MgO surface, Giordano et al.[39] reported that the average binding energy per molecule of water in the monolayer coverage is nearly twice as large as that of an isolated molecule, namely 58.1 and 33.0 kJ/mol, respectively. These values can be compared to experimental data of 84.9 ± 2.1 and 50.2 ± 10.0 kcal/mol, respectively.[52] Our calculated value from the water dimer is noticeably smaller than that corresponding to the monolayer coverage. This is due to the fact that in an adsorbed water dimer, there is only one neighboring water molecule around any center water, whereas there are six neighboring water molecules around any center water molecule in Giordano's 3 × 2 water monolayer model. In addition, cooperative effects between coadsorbed water molecules existed in previous periodic studies and were not included in our study of the adsorption of a water dimer.

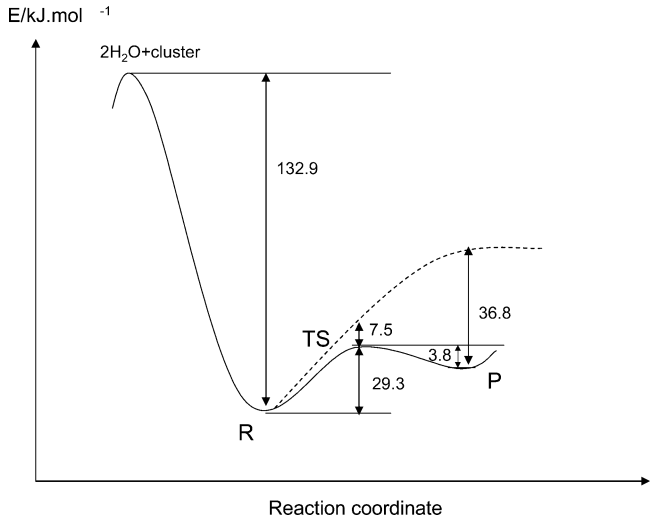

Figure 3. Schematic energy profile (solid curve) for dissociation of water dimer on the MgO(100) surface. Numerical values are from the IMOMO (CCSD:HF) calculations. Dashed curve is for isolated water using the dimer configuration in which the coadsorbed water is removed. R and P denote the molecular adsorption and dissociative chemisorption complexes, respectively. Dashed curve is superimposed with the solid curve at R to facilitate comparison.

The classical forward barrier for the dissociative chemisorption of a water molecule in the presence of a coadsorbed water molecule is 29.26 kJ/mol, and the corresponding reverse barrier is 3.80 kJ/mol (see Table 2 and Figure 3). These results indicate that single coadsorbed water is sufficient to stabilize the water dissociated hydroxyl species on the perfect MgO(100) surface to become a local stable structure on the potential energy surface. However, the reverse barrier vanishes when zero-point energy corrections are included. Thus, one would not expect to observe dissociation of the isolated water dimer on the perfect MgO(100) surface experimentally. Though by extrapolating from the present results one would expect that increasing the number of coadsorbed water molecules would further stabilize the hydroxyl species and it becomes "theoretically" detectable when it is a local minimum on the free energy surface. We can estimate the degree of stabilization due to coadsorption along the dissociation pathway in the dimer case by also calculating the energy profile using the same geometrical configurations as that of the dimer but the coadsorbed water molecule is removed. The results are also shown in Figure 3. The differences between these two energy profiles give the degree of stabilization by the coadsorbed water along the dissociation coordinate. We found that the coadsorbed water molecule stabilizes the TS by 7.32 kJ/mol and the dissociative hydroxyl species by 36.70 kJ/

mol. One can expect that the degree of stabilization for adding the second coadsorbed water would be smaller. Furthermore, judging from the difference between this degree of stabilization at the dissociative product and at the transition state, one can guesstimate that two coadsorbed water molecules would be sufficient to yield a 'theoretically' detectable hydroxyl species. Unfortunately, studying adsorption of a water trimer would require a substantially larger MgO cluster to avoid edge effects and thus the same level of theory would require computing resources that is beyond our current capability. However, our results support the dissociation process of partial water on the perfect MgO surface that was observed in the recent experiment.[36] In addition, because of the small reverse barrier, a reverse process of a dissociation path also occurs easily. In other words, a desorption process of water dissociated from the surface can easily happen in the molecular form as suggested by Giordano et al.[42]

It is also interesting to analyze the relative importance of the effects of electron correlation and Madelung potential on the dissociative chemisorption process. Such information is quite useful in designing the appropriate physical model and choosing a sufficiently accurate level of theory for studying chemical processes on metal oxide surfaces. By comparisons between the calculated barriers and reaction energies at the CCSD and HF levels using the small cluster model with the same geometries that were optimized at the HF level with the embedded cluster model described above, we found that the electron correlation raises the barrier 0.71 kJ/mol whereas the reaction energy is changed by 20.77 kJ/mol. Thus, the electron correlation is more important in the molecular adsorbed dimer complex than in the hydroxyl species. Hence, it is also important in calculating the binding energy of the adsorbed complex. In fact, this was verified in the study of adsorption of an isolated water molecule discussed in the previous section. To estimate the importance of the Madelung potential, we compare HF results calculated using the embedded cluster and bare cluster models using the same geometries as above. Interestingly, we found that the Madelung potential lowers the dissociation barrier by 22.99 kJ/mol and the reaction energy by 8.53 kJ/mol. In other words, the Madelung potential as expected is more important at the transition state and the product hydroxyl species. In summary, electron correlation has a large effect on the molecular adsorption whereas the Madelung potential plays an important role in stabilizing the transition state and the dissociative chemisorption product.

2.3. Analysis of Density of State Spectra. In our recent study on the effects of surface interactions and thermal fluctuations on the electronic spectrum of isolated water adsorbed on the perfect MgO(100) surface,[53] we found that both of these effects introduce only small shifts to the water orbital energies. This fact supported the experimental interpretation that the new peak in the MIES spectra[36] of water on the MgO(100) surface is due to the hydroxyl species resulted from the water dissociation.

To analyze the electronic structure characteristics of the dissociation of a water dimer on the perfect MgO(100) surface, we have performed similar analyses to our previous study[53] on the electronic spectra of both the molecular and dissociative adsorption complexes. Figure 4 shows plots of the densities of states (DOS) based on the embedded HF calculations. For an isolated water molecule, the orbital symmetry order of increasing energy is $1b_2$, $3a_1$, and $1b_1$ for the three valence orbitals.[35] As the adsorbed water dimer proceeds from the molecular adsorption complex to its dissociative form, the b_2 peak is disappearing. While two new peaks associated with the σ-type and π-type orbitals of H−O species are growing. The σ-type orbital population is contributed by the p orbital of the oxygen atom and the s orbital of the hydrogen atom of an H−O ion. The π-type orbital population is contributed by an isolate-electron-pair of the oxygen atom of the hydroxyl. The calculated peak separations are given in Table 3 along with the experimental values from the MIES spectra obtained by Kim et al.[35] The calculated peak separations between 1b2−3a1 and 3a1−1b1 for the molecular adsorbed case are 4.0 and 1.6 eV, as compared to experimental values of 4.3 and 2.0 eV, respectively. For the dissociative complex, the calculated separation between $\sigma-\pi$ peaks is 4.0 eV which is in excellent agreement of the MIES experimental value as well. These comparisons further support

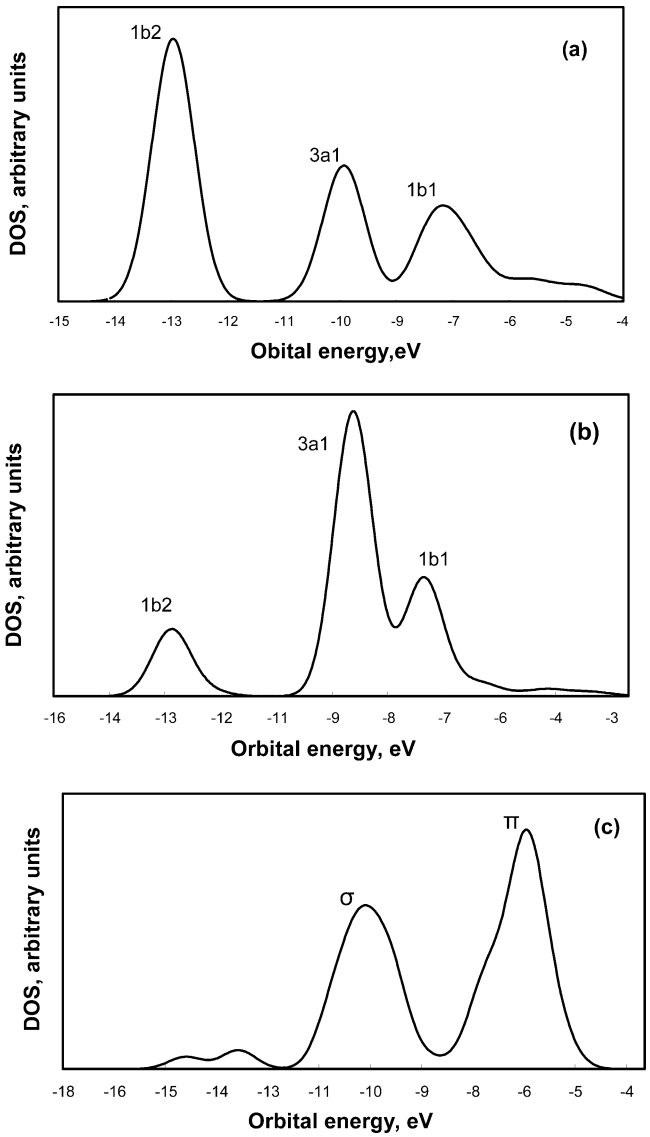

Figure 4. Plots of partial density of state of water adsorption on the MgO (100) surface (a) for the isolated water; (b) for the molecular adsorbed dimer complex; (c) for the dissociative dimer complex.

TABLE 3: Peak Separations (eV) of Electronic Spectra of Isolated Water and Water Dimer on the MgO(100) Surface

	ΔE	theory	expt[36]
1 H_2O	1b2−3a1	3.4	
adsorption	3a1−1b1	1.9	
2 H_2O	1b2−3a1	4.0	4.3
adsorption	3a1−1b1	1.6	2.0
	$\sigma-\pi$	4.0	4.4

the interpretations of the MIES spectra for evidence of water dissociation on the MgO(100) surface.[36,41]

Conclusions

We have carried a systematic theoretical study on the effects of coadsorption on the mode of adsorption of water on the perfect MgO(100) surface. In particular, the dissociative pathway of a water dimer on this MgO single-crystal surface was investigated using the ab initio embedded cluster methodology. To improve the energetic properties, the IMOMO (CCSD:HF) method was employed. We confirmed previous findings that isolated water can only molecularly be adsorbed on the perfect MgO(100) surface with the binding energy of about 58.02 kJ/mol which is within the experimental uncertainty and also consistent with previous theoretical calculations. These results validate the methodology and level of theory employed in this study. We found that interaction with an additional water molecule can help to stabilize the dissociative product, the hydroxyl species. However, it is 25.5 kJ/mol above the molecular adsorbed complex and has a relatively low barrier of 3.8 kJ/mol for association (the reverse reaction). When zero-point energy corrections are included, we found that the hydroxyl species in the water dimer complex can readily convert back to the more stable molecularly adsorbed dimer. Analysis on the degree of stabilization due to coadsorbed molecules showed that the coadsorbed water molecule can stabilize the hydroxyl species by 36.8 kJ/mol. Adding more coadsorbed water molecules is expected to lower the relative energy of the dissociative complex. "Theoretically", one can extrapolate the present results to infer that two coadsorbed water molecules would be sufficient to yield observable hydroxyl species, i.e., stable species on the free energy surface. Analysis on the electronic spectra further confirms that the peak located near 6 eV is due to the π-orbital of the hydroxyl species and thus suppors the MIES interpretation of dissociation of water on the perfect MgO(100) surface in the submonolayer coverage range.

Acknowledgment. This work is supported by the National Science Foundation. We also acknowledge computing resources provided by the University of Utah Center for High Performance Computing.

References and Notes

(1) de Leeuw, N. H.; Watson, G. W.; Parker, S. C. *J. Phys. Chem.* **1995**, *99*, 17219.
(2) Beruto, D.; Searcy, A. W.; Botter, R.; Giordani, M. *J. Phys. Chem* **1993**, *97*, 9201.
(3) Langel, W.; Parrinello, M. *Phys. Rev. Lett.* **1994**, *73*, 504.
(4) Dunski, H.; Jozwiak, W. K.; Sugier, H. *J. Catal.* **1994**, *146*, 166.
(5) Komiyama, M.; Gu, M. *Appl. Surf. Sci.* **1997**, *120*, 125.
(6) Daniels, B. G.; Lindsay, R.; Thornton, G. *Surf. Rev. Lett.* **2001**, *8*, 95.
(7) de Leeuw, N. H. *J. Phys. Chem. B* **2001**, *105*, 9747.
(8) Picaud, S.; Toubin, P. N.; Hoang, N.; Girardet, C. *Surf. Sci.* **2002**, *502*−*503*, 268.
(9) Johnson, M. A.; Stefanovich, E. V.; Truong, T. N.; Gunster, G.; Goodman, D. W. *J. Phys. Chem. B* **1999**, *103*, 3391.
(10) Thiel, P. A.; Madey, T. E. *Surf. Sci. Rep.* **1987**, *7*, 211.
(11) Ferry, D.; Picaud, S.; Hoang, P. N. M.; Girardet, C.; Giordano, L.; Gemirdjian, B.; Buzanne, J. *J. Surf. Sci.* **1998**, *409*, 101.
(12) Xu, C.; Goodman, D. W. *Chem. Phys. Lett.* **1997**, *265*, 341.
(13) Heidberg, J.; Redlich, B.; Wetter, D.; Bunsen-Ges, B. *Phys. Chem.* **1995**, *99*, 1333.
(14) Goodman, A. L.; Bernard, E. T.; Grassian, V. H. *J. Phys. Chem. A* **2001**, *105*, 6443.
(15) Demirdjian, B.; Suzanne, J.; Ferry, D.; Coulomb, J. P.; Giordano, L. *Surf. Sci.* **2000**, *462*, L581.
(16) Ferry, D.; Glebov, A.; Senz, V.; Suzanne, J.; Toennies, J. P.; Weiss, H. *Surf. Sci.* **1997**, *377*−*379*, 634.
(17) Ferry, D.; Glebov, A.; Senz, V.; Suzanne, J.; Toennies, J. P.; Weiss, H. *J. Chem. Phys.* **1996**, *105*, 1697.
(18) Langel, W. *J. Mol. Struct.* **1995**, *349*, 69.
(19) Evans, J. V.; Whateley, T. L. *Trans. Faraday Soc.* **1967**, *63*, 2769.
(20) Webster, R. K.; Jones, T. L.; Anderson, P. J. *Proc. Brit. Ceram. Soc.* **1965**, *5*, 153.
(21) Stefanovich, E. V.; Truong, T. N. *J. Phys. Chem. B* **1998**, *102*, 3018.
(22) Stefanovich, E. V.; Truong, T. N. *J. Chem. Phys.* **1996**, *104*, 22.
(23) Ahdjoudj, J.; Markovits, A.; Minot, C. *Catal. Today* **1999**, *50*, 541.
(24) Tikhomirov, V. A.; Geudtner, G.; Jug, K. *THEOCHEM* **1999**, *458*, 161.
(25) Russo, S.; Noguera, C. *Surf. Sci.* **1992**, *262*, 259.
(26) Russo, S.; Noguera, C. *Surf. Sci.* **1992**, *262*, 245.
(27) Scamehorn, C. A.; Harrison, N. M.; Mccarthy, M. I. *J. Chem. Phys.* **1994**, *101*, 1547.
(28) Almeida, A. L.; Martins, J. B. L.; Longo, E.; Furtado, N. C.; Taft, C. A.; Sarnbrano, J. R.; Lester, W. A., Jr. *Int. J. Quantum Chem.* **2001**, *84*, 705.
(29) Almeida, A. L.; Martins, J. B. L.; Taft, C. A.; Longo, E.; Lester, W. A., Jr. *Int. J. Quantum Chem.* **1999**, *71*, 153.
(30) Marmier, A.; Hoang, P. N. M.; Picaud, S.; Girardet, C. *J. Chem. Phys.* **1998**, *109*, 3245.
(31) Langel, W.; Parrinello, M. *J. Chem. Phys.* **1995**, *103*, 3240.
(32) Liu, P.; Kendelewicz, T.; Brown, G. E., Jr.; Parks, G. A. *Surf. Sci.* **1998**, *412*, 287.
(33) Almerida, A. L.; Martins, J. B. L.; Taft, C. A.; Lester, W. A., Jr. *J. Chem. Phys.* **1998**, *109*, 3671.
(34) Lynden-Bell, R. M.; Site, L. D.; Alavi, A. *Surf. Sci.* **2002**, *496*, 1.
(35) Wu, M. C.; Estrada, C. A.; Corneille, J. S.; Goodman, D. W. *J. Chem. Phys.* **1992**, *96*, 3892.
(36) Kim, Y. D.; Stulz, J.; Goodman, D. W. *J. Phys. Chem. B* **2002**, *106*, 1515.
(37) Site, L. D.; Alavi, A.; Lynden-Bell, R. M. *J. Chem. Phys.* **2000**, *113*, 3344.
(38) Odelius, M. *Phys. Rev. Lett.* **1999**, *82*, 3919.
(39) Giordano, L.; Goniakowski, J.; Suzanne, J. *J. Phys. Rev. Lett.* **1998**, *81*, 1271.
(40) Tikhomirov, V. A.; Jug, K. *J. Phys. Chem. B* **2000**, *104*, 7619.
(41) Kim, Y. D.; Lynden-Bell, R. M.; Alavi, A.; Stulz, J.; Doodman, D. W. *Chem. Phys. Lett.* **2002**, *352*, 318.
(42) Giordano, L.; Goniakowski, J.; Suzanne, J. *Phys. Rev. B* **2000**, *62*, 15406.
(43) Stefanovich, E. V.; Truong, T. N. *J. Phys. Chem. B* **1998**, *102*, 3018.
(44) Treesukol, P.; Lewis, J. P.; Limtrakul, J.; Truong, T. N. *Chem. Phys. Lett.* **2001**, *350*, 128.
(45) Shapovalov, V.; Truong, T. N. *J. Phys. Chem. B* **2000**, *104*, 9859.
(46) Boys, S. F.; Bernardi, F. *Mol. Phys.* **1970**, *19*, 553.
(47) Frisch, M. J.; Trucks., G. W.; Schlegel, H. B.; Scuseria, G. E.; Robb, M. A.; Cheeseman, J. R.; Zakrzewski, V. G.; Montgomery, J. A., Jr.; Stratmann, R. E.; Burant, J. C.; Dapprich, S.; Millam, J. M.; Daniels, A. D.; Kudin, K. N.; Strain, M. C.; Farkas, O.; Tomasi, J.; Barone, V.; Cossi, M.; Cammi, R.; Menucci, B.; Pomelli, C.; Adamo, C.; Clifford, S.; Ochterski, J.; Petersson, G. A.; Ayala, P. Y.; Cui, Q.; Morokuma, K.; Malick, D. K.; Rabuck, A. D.; Raghavachari, K.; Foresman, J. B.; Cioslowski, J.; Ortiz, J. V.; Baboul, A. G.; Stefanov, B. B.; Liu, G.; Liashenko, A.; Piskorz, P.; Komaromi, I.; Gomperts, R.; Martin, R. L.; Fox, J.; Keith, T.; Al-Laham, M. A.; Peng, C. Y.; Nanayakkara, A.; Gonzalez, C.; Challacombe, M.; Gill, P. M. W.; Johnson, B.; Chen, W.; Wong, M. W.; Andres, J. L.; Gonzalez, C.; Head-Gordon, M. E.; Replogle, S.; Pople, J. A. *Gaussian 98*, Revision A.7; Gaussian, Inc: Pittsburgh, PA 1998.
(48) McCarthy, M. I.; Schenter, G. K.; Scamehorn, C. A.; Nicholas, J. B. *J. Phys. Chem.* **1996**, *100*, 16989.
(49) Wu, M. C.; Goodman, D. W. *Catal. Lett.* **1992**, *15*, 1.
(50) Ferrari, A. M.; Giordano, L.; Rosch, N.; Heiz, U.; Abbet, S.; Sanchez, A.; Pacchioni, G. *J. Phys. Chem.* **2000**, *104*, 10612.
(51) Joyce, S.; Kay, B. *J. Chem. Phys.* **1996**, *105*, 1295.
(52) Ferry, D.; Girardet, C.; Suzanne, J. *Surf. Sci.* **1998**, *409*, 101.
(53) Shapovalov, V.; Wang, Y.; Truong, T. N. *Chem. Phys. Lett.* **2003**, *375*, 321.